# Dynamic Viscoelasticity of Actin Networks Cross-Linked with Wild-Type and Mutant $\alpha$-Actinin-4

by

Sabine M. Volkmer Ward

Diplom Physics, Friedrich-Schiller-Universität Jena, 2005

Submitted to the Department of Physics
in partial fulfillment of the requirements for the degree of

Master of Science

at the

MASSACHUSETTS INSTITUTE OF TECHNOLOGY

February 2008



Author .....

Department of Physics
Feb 1, 2008

Certified by ....

David A. Weitz
Professor of Physics and of Applied Physics, Harvard University
Thesis Supervisor

Certified by

Alexander van Oudenaarden
Associate Professor of Physics
Thesis Supervisor

Accepted by .....

Thomas J. Greytak
Associate Department Head for Education

# Dynamic Viscoelasticity of Actin Networks Cross-Linked with Wild-Type and Mutant $\alpha$-Actinin-4

by

Sabine M. Volkmer Ward

Submitted to the Department of Physics
on Feb 1, 2008, in partial fulfillment of the
requirements for the degree of
Master of Science

## Abstract

The actin cross-linker $\alpha$-actinin-4 has been found indispensable for the structural and functional integrity of podocytes; deficiency or alteration of this protein due to mutations disturbs the cytoskeleton and results in kidney disease. This thesis presents rheological studies of in vitro actin networks cross-linked with wild-type and mutant $\alpha$-actinin-4, which provide insight into the effect of the cross-linker on the mechanical properties of the networks.

The frequency dependent viscoelasticity of the actin/$\alpha$-actinin-4 networks is characterized by an elastic plateau at intermediate frequencies, and relaxation towards fluid properties at low frequencies. Since the elastic plateau is a consequence of cross-linking, its modulus increases with the $\alpha$-actinin-4 concentration. Networks with wild-type and mutant $\alpha$-actinin-4 differ significantly in their time scales: The relaxation frequencies of networks with the mutant cross-linker are an order of magnitude lower than that with the wild-type, suggesting a slower dissociation rate of mutant $\alpha$-actinin-4 from actin, consistent with a smaller observed equilibrium dissociation constant. This difference can be attributed to an additional binding site, which is exposed as a result of the mutation. An increase in the temperature of networks with mutant $\alpha$-actinin-4 appears to return the viscoelasticity to that of networks cross-linked by the wild-type. Moreover, the temperature dependence of the relaxation frequencies follows the Arrhenius equation for both cross-linkers. These results strongly support the proposition that the macroscopic relaxation of the networks directly reflects the microscopic dissociation rates of their constituents.

Thesis Supervisor: David A. Weitz
Title: Professor of Physics and of Applied Physics, Harvard University

Thesis Supervisor: Alexander van Oudenaarden
Title: Associate Professor of Physics

# Acknowledgments

I would like to thank my research advisor, David Weitz, and his group at the School of Engineering and Applied Sciences at Harvard University, for providing a stimulating and supportive environment in which the work presented in this thesis could thrive. Dave has provided insight and numerous fruitful suggestions for this project. Moreover, his enthusiasm, direct criticism, and genuine support foster a great work atmosphere in the group and beyond, which makes research exciting and enjoyable. I would also like to thank my co-supervisor, Alexander van Oudenaarden from MIT, for his support.

This research is the result of a collaboration with several colleagues at Harvard Medical School. I am particularly grateful to Astrid Weins and Martin Pollak, who introduced me to the medical findings which motivated my rheological studies of wild-type and mutant $\alpha$-actinin-4, provided me with these proteins, and finally discussed my results. Further, I would like to thank Fumihiko Nakamura from Thomas Stossel's group for purifying the actin I used, and answering all my biochemical questions promptly and most helpfully. I thank Bill Brieher from Tim Mitchison's lab for providing chicken gizzard $\alpha$-actinin for comparative measurements.

My work has benefited from the help and hints of many "Weitzlab" members. Special thanks go to Karen Kasza and Dan Blair, who performed the precursor experiments for my project, and gave me much good advice throughout. I am also indebted to the members of our Biophysics Working Group as well as the frequent occupants of the rheology lab, whose ideas and problem solving skills have accelerated my progress many times.

During my stay at Harvard, I have had the opportunity to explore a variety of techniques in the broader context of my research. I am very grateful to Claudia Friedsam for sharing her expertise in Atomic Force Microscopy with me, and to Hans Wyss for showing me how to study macroscopic forces with a beautifully simple microaspiration setup. Further, I would like to acknowledge the kind help of Martin Vogel, Richard Schalek, and Jiandong Deng, who provided assistance with the Confocal Microscope and AFM at the Harvard Center for Nanoscale Systems.

Finally, I would like to thank my husband, David Ward, who is an inexhaustible source of intellectual stimulation and adventure, and our families in Germany and Texas, visiting whom always reminds me that "there is no place like home".

# Contents

# List of Figures

# Chapter 1

# Introduction

This thesis presents rheological studies of in vitro networks formed of actin and $\alpha$-actinin-4, two physiologically very important proteins. Rheometry, a technique commonly used to measure the deformation and flow properties of soft materials for example in the food, cosmetic, and oil industry, has been discovered over the past decades as a means to investigate the characteristics of biological materials as well [11]. In particular, it has helped to elucidate the mechanical properties of the cytoskeleton and its constituents: actin, microtubules, and intermediate filaments. Recent medical interest in the actin cross-linker $\alpha$-actinin-4, whose lack or mutation has been found to cause kidney disease, has motivated the research presented here [25]. To put the results of these experiments in context, the following sections will provide background information on rheology, actin networks, and $\alpha$-actinin-4 and its critical role for the structural and functional integrity of kidney cells.

## 1.1 Rheology

Rheology (from Greek $\rho\epsilon\omega$ = to flow) is the study of the deformation and flow of soft condensed matter in response to external forces. The term applies generally to both extensional rheology, in which the force per unit area, or stress, is normal to the face of the material, and shear rheology, in which the stress is tangential to the surface. In the following, we will

only deal with shear rheology. We denote the shear stress with $\sigma$, and the resulting shear strain, defined as the tangent of the shear angle, with $\gamma$, as is conventional.

Classically, condensed matter is classified into liquids and solids. When liquids are subjected to shear stress, they flow, i.e. they deform irreversibly, dissipating the deformation energy as heat. In the ideal case of a Newtonian liquid, the rate of deformation, or strain rate $d\gamma/dt$, is proportional to the applied stress:

$$\sigma = \eta \cdot \frac{d\gamma}{dt} \tag{1.1}$$

The constant of proportionality, $\eta$, is the dynamic viscosity of the material, and can be thought of as a measure of liquid friction. Water is a thin liquid with a viscosity of about 1 mPa·s, whereas olive oil is thicker and has a viscosity of 81 mPa·s. Solids under stress deform reversibly until an equilibrium between the external forces and the materials restoring forces is reached. The deformation energy is stored and, for an ideal elastic solid, completely recovered once the external stress is released. Here, the deformation, not its time derivative, is proportional to the applied stress:

$$\sigma = G \cdot \gamma \tag{1.2}$$

The constant of proportionality is the shear modulus $G$. As an example, commercial Jello has a shear modulus of $\sim$100 Pa.

Models that capture the idealized behaviors of a Newtonian liquid and an elastic solid are a dash pot and a Hookian spring, respectively. Many materials we encounter in everyday life, however, do not completely fall in either of these categories. Instead, they exhibit both fluid-like and solid-like behaviors–they are viscoelastic [14]. Illustrative examples of such complex fluids are mayonnaise and peanut butter, shampoo and toothpaste, drilling mud, blood, and liquid crystals. Viscoelastic materials can be modeled by a combination of springs and dash pots. Their deformation, or strain ($\gamma$), generally lags behind the applied stress. Consequently, the ratio between stress and strain can be described by a complex number,

the dynamic modulus $G^*$:

$$\frac{\sigma}{\gamma} = G^* = G' + i\,G'' \tag{1.3}$$

The real part of $G^*$ is the elastic or storage modulus $G'$; the imaginary part is the viscous or loss modulus $G''$. For an ideal elastic solid, stress and strain are in phase, and the dynamic modulus reduces to $G'$. For a Newtonian liquid, stress and strain are exactly 90° out of phase, such that the dynamic modulus reduces to $i\,G''$. The relation between $G^*$ and the viscosity $\eta$ and shear modulus $G$ introduced in equations 1.1 and 1.2 is best illustrated for a sinusoidally oscillating strain:

$$\gamma = \gamma_0 \cdot \exp(i\,\omega\,t) \tag{1.4}$$

$$\frac{d\gamma}{dt} = i\,\omega\,\gamma_0 \cdot \exp(i\,\omega\,t) \tag{1.5}$$

$$\sigma = G' \cdot \gamma + \frac{G''}{\omega}\,i\,\omega\,\gamma = G' \cdot \gamma + \frac{G''}{\omega}\,\frac{d\gamma}{dt} \tag{1.6}$$

It follows that $G' = G$ and $G'' = \eta \cdot \omega$. As we see, the viscous modulus $G''$ is proportional to the frequency of the imposed mechanical perturbations for an ideal liquid of frequency independent viscosity. In general, however, both the viscosity and the elasticity of the network depend on the rate of deformation, as they reflect the properties and typical time scales of structural rearrangements in the material. Taking the imaginary part of equations 1.4 and 1.5, stress and strain are therefore related by:

$$\sigma(t) = \gamma_0\,[G'(\omega)\,\sin(\omega\,t) + G''(\omega)\,\cos(\omega\,t)] \tag{1.7}$$

Matters are further complicated by the fact that the linear viscoelastic response described by equation 1.7 only holds for small perturbations which leave the network properties unaltered. At high stresses, the dynamic modulus can itself be stress dependent. If it increases with stress, leading to a superlinear increase of the applied stress amplitude with the strain amplitude, the material is called stress-stiffening. If, on the other hand, the modulus decreases at high stresses, resulting in a sublinear increase of stress with strain, the material yields

and is described as stress-weakening. In the non-linear regime, a sinusoidally varying stress does not result in a sinusoidal strain any more, and vice versa.

The dynamic modulus of a soft material can be measured with a conventional rheometer, which subjects the sample to a shear stress, and determines the resulting shear strain. Alternatively, the instrument can impose a specific strain or constant shear rate, and measure the resulting stress. These two modes of operation are referred to as stress- and strain-controlled, respectively. Rheometers can control shear stress over a large range, from 0.01 Pa to 10 kPa, which, for soft materials, extends well into the non-linear regime. The sample is typically loaded into a cylinder-symmetric geometry, such as the space between to concentric cylinders, or between two horizontal plates. For the experiments described later on in this thesis, a cone and plate geometry, as illustrated in Fig. 1-1(a), was used. Through rotation of the conical tool around its axis, a torsional shear stress is applied to the sample. This specific geometry bears the advantage of admitting uniform shearing: If a tool with cone angle $\delta$ rotates by an angle $\phi$, a cylindrical ring of the sample with radius $r$ and height $h(r)$ experiences a shear strain

$$\gamma = \phi \cdot \frac{r}{h(r)} = \frac{\phi}{\tan\delta}, \tag{1.8}$$

which is independent of its radius (Fig. 2b). The shear stress is likewise uniform across the sample, and results in a differential force

$$dF(r) = \sigma \cdot 2\pi\, r\, dr \tag{1.9}$$

and a torque

$$\tau = \int_0^R r\, dF(r) = \frac{2\pi}{3}\, \sigma\, R^3, \tag{1.10}$$

where $R$ is the radius of the tool. From the exerted torque $\tau$ and the resulting angular displacement $\phi$ of the tool, the instrument computes stress and strain according to equations 1.8 and 1.10.

Rheometry can be static or oscillatory. An example of the former is a creep experiment, in which a constant shear stress is applied, and the transient strain or strain rate is monitored

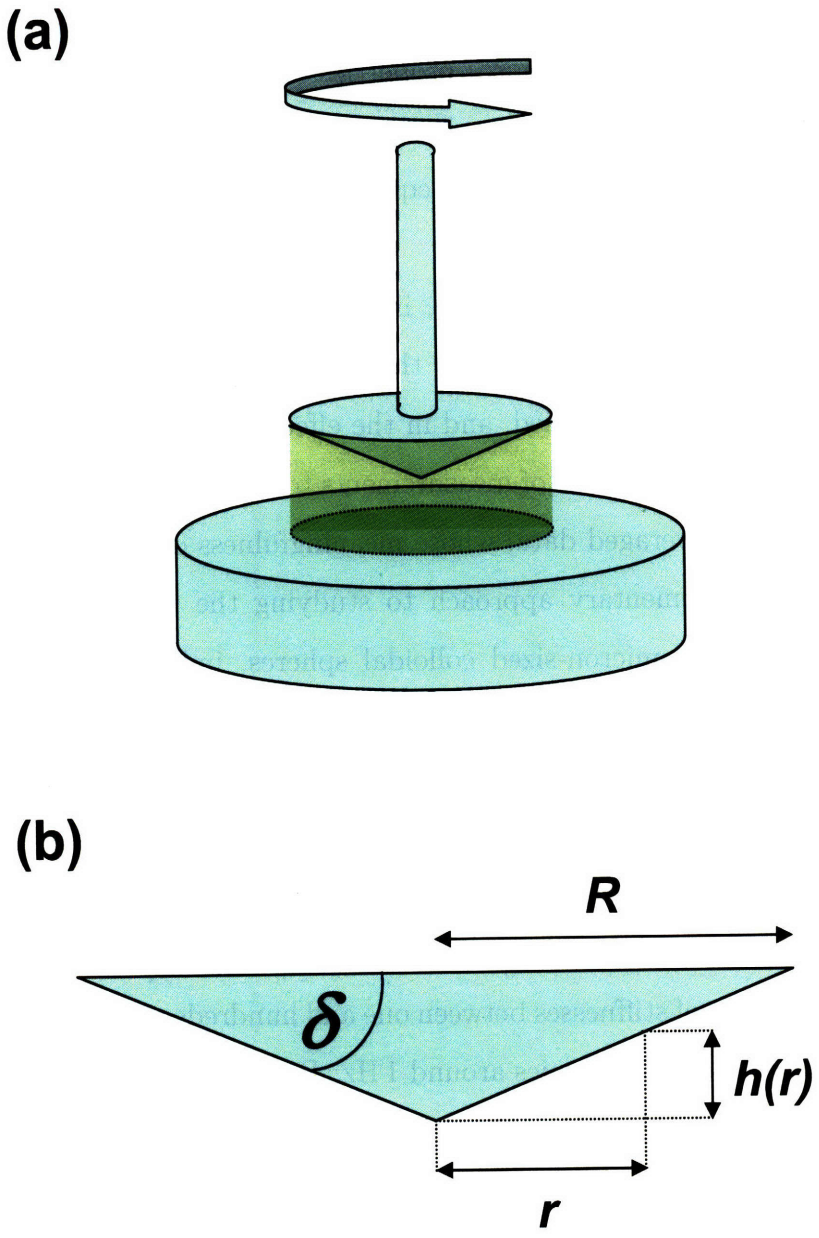


Figure 1-1: Rheology with a cone and plate geometry. (a) The sample is loaded between the lower plate and a conical tool, which rotates around its axis. (b) Definition of quantities used in equations 1.8, 1.9, and 1.10. The dimensions are not drawn to scale; cone angle and gap size are exaggerated for clarity.

over time. After removal of the applied stress, the relaxation of the material can be observed similarly. For liquid-like materials, the shear rate is often held constant, and the time dependent stress is measured until a steady stress is reached. These types of experiments provide information about the rheological properties on long time scales. Here, we present the results of small-amplitude oscillatory rheology, and focus on the frequency dependence of the linear viscoelasticity, as described by equation 1.7, for frequencies between 0.01 and 10 Hz.

The limitations of conventional rheology, in particular when applied to biological materials, lie in the need for sample volumes that are large compared with the quantities in which proteins are typically purified, and in the effects of sample drying and protein denaturation, which limit the duration of measurements to several hours. Further, bulk rheology provides only sample-averaged data, whose meaningfulness depends on the homogeneity of the sample. A complementary approach to studying the properties of soft materials is microrheology, in which micron-sized colloidal spheres, imbedded in the material and optically tracked, probe the local thermal strain fluctuations of the network. Microrheology bears the advantages of higher accessible frequencies (up to $10^5$ Hz) and smaller sample volumes. However, it is practically limited to samples with elastic moduli of no more than 10 Pa, and the interpretation of the thermal motion of the tracer colloids can be complicated through heterogeneities in the network microstructure. The actin/$\alpha$-actinin networks studied in this thesis span a range of stiffnesses between one and hundreds of Pascals, and exhibit very interesting features at shear frequencies around 1 Hz. Bulk rheology therefore constitutes an adequate method for the investigation of their viscoelastic properties.

## 1.2 Actin networks

Cells owe their shape, spatial organization, motility, adhesion, and mechanical stability to an intricate network of interconnected filamentous proteins, called the cytoskeleton [1]. The major building blocks of the cytoskeleton are three types of polymers, each assembling into characteristic structures and carrying typical functions: Actin filaments form bundles and

networks close to the cell membrane, which determine the cell shape and enable cell locomotion with the help of surface protrusions. In muscle cells, they arrange in parallel with myosin to build long, contractile fibers. Microtubules often occur in a star-like configuration and are responsible for the positioning and intracellular transport of cell organelles. Intermediate filaments, which can be grouped into several families located in different cell types, provide mechanical stability and resistance to shear stress and pressure.

In an attempt to gain further insight into the mechanical properties of cells and the cytoskeleton, researchers have studied two types of systems: the cells themselves, and model networks formed of individual cytoskeletal components in vitro [11]. Much research in recent years has focused on reconstituted networks of actin–one of the most abundant proteins in eukaryotic cells. Filamentous actin, or F-actin, is a polymer composed of 42 kDa globular monomeric subunits called G-actin. At physiological salt concentrations, G-actin self-assembles into double-stranded, helical, semiflexible micro-filaments with a 72 nm pitch and a filament diameter of approximately 7 nm [17]. Actin filaments are polarized, dynamic structures. In equilibrium, they assemble at one end and disassemble at the other end, reaching lengths of typically $20\,\mu$m. The persistence length of actin filaments, defined as the length over which correlations in the tangent vector to the filament contour are lost, is comparable ($\sim 17\,\mu$m) [4]. Therefore, actin filaments behave neither as rigid rods nor as completely flexible polymers; they are semiflexible, and their thermal bending fluctuations contribute to the network properties, in particular at short time scales.

Purified actin polymerized in vitro at concentrations of $\sim$1 mg/ml forms finely meshed entangled networks, as shown by confocal microscopy of fluorescently labeled actin (Fig. 3-1(a)). Rheologically, these networks behave like weak viscoelastic solids. Upon initialization of the polymerization reaction, the network stiffness increases rapidly over a few up to tens of minutes, reflecting the growing fraction of polymerized actin, and then starts leveling off (Fig. 1-2(a)). The elastic modulus of the final network is only weakly frequency dependent over a large range (Fig. 1-2(b)). It typically assumes values on the order of 0.1 Pa to 1 Pa. While two orders of magnitude higher moduli have been reported for entangled actin, consensus has

been reached that this discrepancy is largely a consequence of protein aging under unsuitable storage conditions [26], and partly a result of traces of actin-binding proteins that may exist as impurities in the solutions, as well as of repeated mechanical perturbations during measurements [9]. The data presented in Fig. 1-2 are taken on actin samples prepared under the same conditions as those studied later on in this thesis, up to the deliberate addition of cross-linkers to the latter, and serve for comparisons of pure and cross-linked networks.

The actin cytoskeleton in cells is orders of magnitude stiffer than pure entangled actin networks in vitro, suggesting that cross-linking is essential in inducing physiologic network properties. In vivo, a myriad of cross-linker, motor, and other actin binding proteins regulate the dynamic actin polymerization and the formation of higher order structures [1, 2]. This complexity renders the detailed understanding of the actin cytoskeleton extremely difficult. Researchers therefore typically limit their in vitro studies of reconstituted actin networks to the investigation of one or two regulatory proteins and their effect on the network properties. One such accessory protein is scruin, a rod-like, rigid 102 kDa molecule, which cross-links and bundles actin irreversibly into isotropic, homogeneous three-dimensional networks. At molar ratios of scruin to actin monomers from 0 and 1, scruin increases the elastic modulus of these networks over three orders of magnitude [7, 19]. Since scruin itself does not contribute to the network compliance, actin-scruin networks serve as a model system for studying the network elasticity that result from the properties of individual actin filaments. Two prominent and physiologically relevant compliant cytoskeletal proteins are filamin and $\alpha$-actinin. Filamin is a hinged dimer of 560 kDa with two actin binding domains, which cross-links actin microfilaments into orthogonal networks. At physiological molar ratios to actin of 0.01 to 0.02, filamin does not affect the linear elasticity of the network much; however, it results in drastic strain stiffening, that is, a remarkable increase in the differential elastic modulus, $K = \Re(d\sigma/d\gamma)$, at strains above 10% [5, 6]. Fig. 1-3(a) shows the linear viscoelastic response of pure entangled actin, and networks cross-linked with scruin (red circles) and filamin (green triangles), illustrating the different effects of the two cross-linkers on the linear network properties.

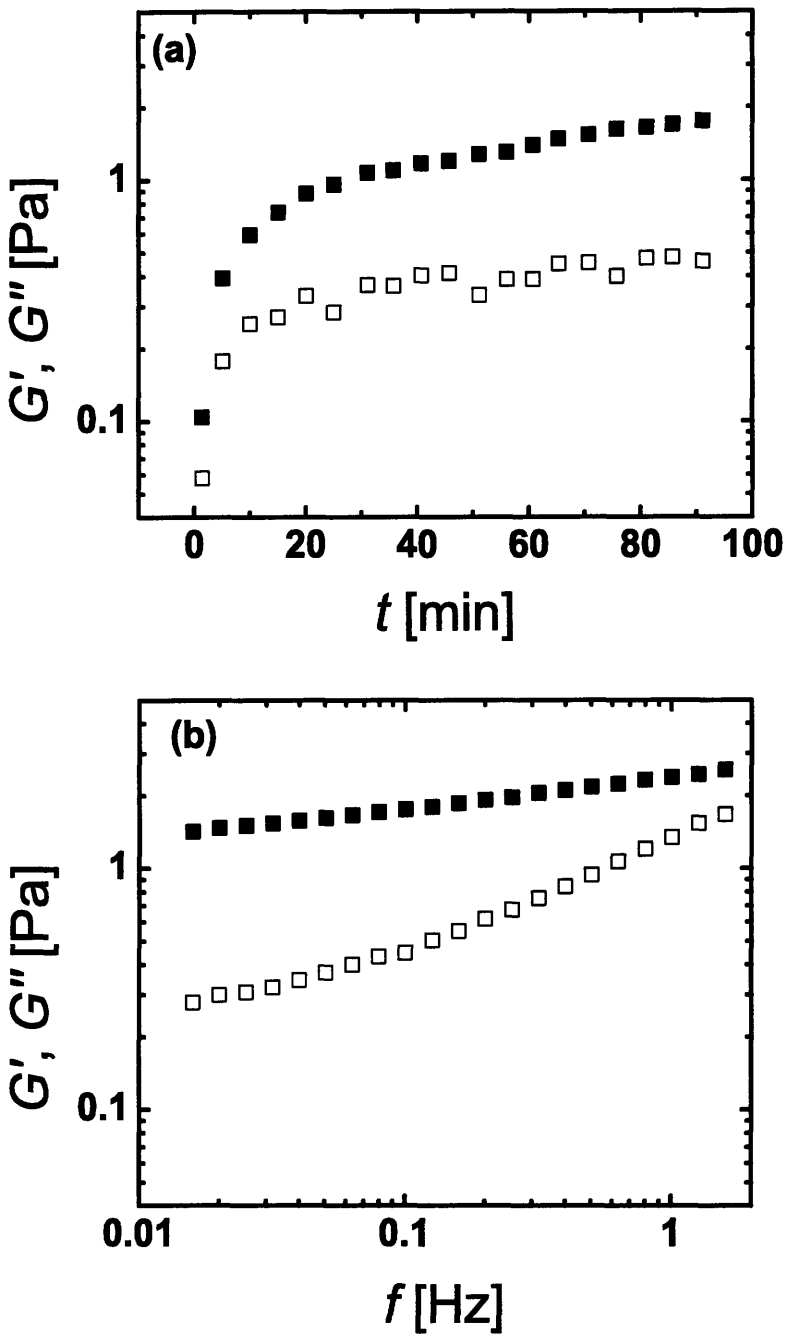


Figure 1-2: Elastic modulus $G'$ (solid squares) and viscous modulus $G''$ (open squares) of entangled actin (1 mg/ml). (a) Moduli as a function of time after initialization of the polymerization reaction, measured at a frequency of 0.1 Hz and a strain of 0.005. The network stiffness levels off after about 30 minutes. (b) Frequency dependent viscoelasticity of the network, measured at a strain of 0.02. The elastic modulus is depends only weakly on the frequency.

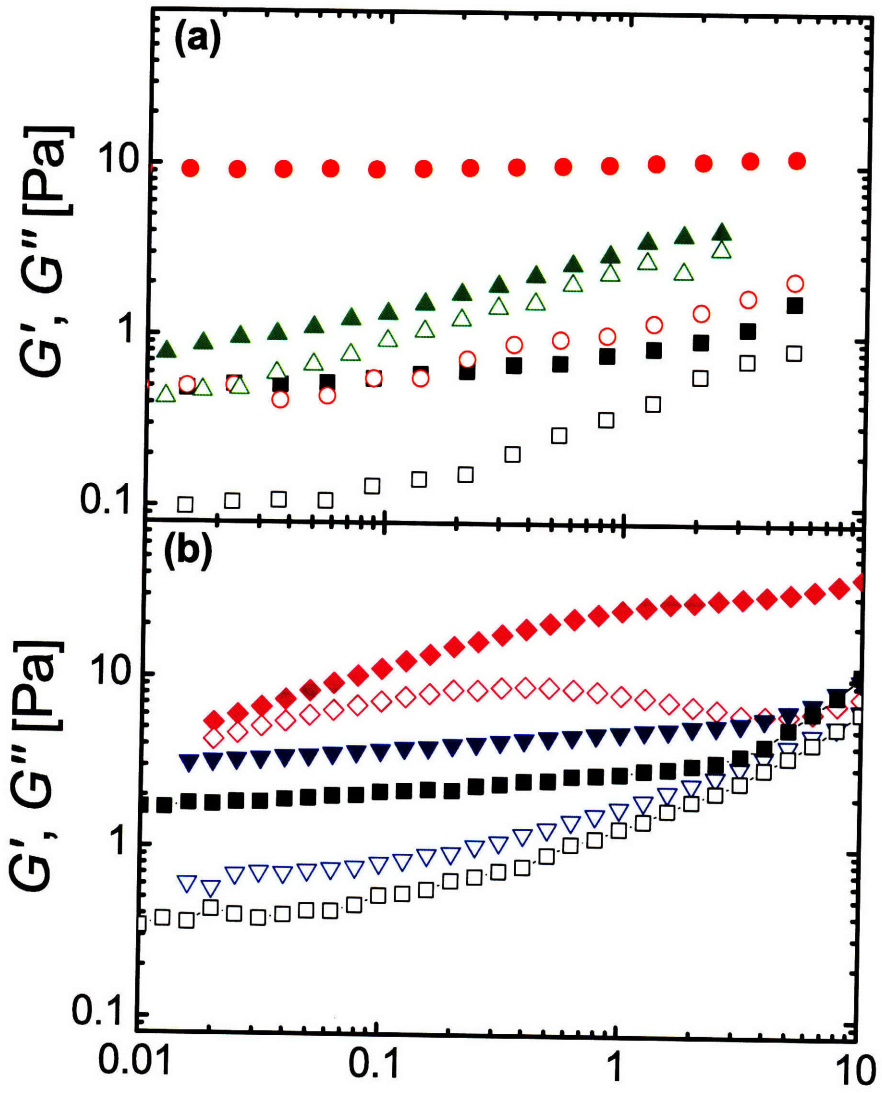


Figure 1-3: Frequency dependent viscoelasticity of networks of actin (1 mg/ml) with and without cross-linkers. (a) Pure entangled actin (black squares), courtesy of Karen Kasza; actin with filamin at a molar ratio $R = 0.01$ (green triangles), courtesy of Karen Kasza; actin with scruin at $R = 0.02$ (red circles), courtesy of Gijsje Koenderink. (b) Pure entangled actin (black squares); actin with chicken-gizzard $\alpha$-actinin at $R = 0.01$ (blue inverted triangles); actin with human $\alpha$-actinin-4 at $R = 0.01$ (magenta diamonds). All samples in (b) are prepared with actin from the same batch.

The antiparallel homodimer $\alpha$-actinin falls somewhere in between scruin and filamin regarding its molecular size and structure. It weighs 200 kDa and measures 40 nm in length, is a rigid rod like scruin, but binds reversibly to actin at its two diametric binding sites like filamin. Depending on its concentration, $\alpha$-actinin can cross-link or bundle actin filaments [21], or form networks of bundles with mesh sizes on the order of the persistence length of actin [18]. Compared with other cross-linkers, it tends to cause greater network inhomogeneities. The various isoforms of the cross-linker, which can be found in smooth muscle, skeletal muscle, and non-muscle cells, result in networks of widely varying viscoelastic properties [21, 27, 20]. Chicken gizzard $\alpha$-actinin, for example, increases the stiffness of entangled actin only slightly, whereas $\alpha$-actinin-4, one of the four isoforms found in mammals, drastically alters the frequency dependent viscoelasticity, as shown in Fig. 1-3(b). The actin binding dynamics of $\alpha$-actinin in its effect on the network properties has been studied by several authors with chicken and turkey gizzard as well as Acanthamoeba $\alpha$-actinin [21, 27, 20, 22]. Recently, human $\alpha$-actinin-4 has gained the attention of medical scientists in the context of research on kidney disease.

## 1.3 Mutant $\alpha$-actinin-4 and its implications for kidney function

Deficiency or mutations of the gene that encodes $\alpha$-actinin-4 can cause Focal and Segmental Glomerulosclerosis (FSGS), a pattern of renal injury, which is characterized by increased urinary protein excretion and slowly progressive kidney dysfunction [10, 12, 15, 24]. An estimated 4% of familial FSGS in affected humans are accounted for by these mutations [24]. Tissue damage is often a consequence of the collapse of glomeruli–renal capillary tufts which serve blood filtration through a three-layered system comprised of endothelium, glomerular basal membrane, and epithelium. Glomeruli are subject to high blood pressures that aid in the process of ultrafiltration; moreover, glomerular hypertension has been established as a source of renal failure. Research on kidney disease has therefore included investigations of

the mechanical properties of glomeruli and the filtration barrier [13, 3].

In $\alpha$-actinin-4 mediated FSGS, the epithelial podocytes are believed to be the initial sites of injury [12]. Podocytes form an interdigitating network of foot processes, which is a major constituent in the filtration barrier, and are exposed to significant mechanical stress due to changes in glomerular capillary pressure. In these cells, $\alpha$-actinin-4, which is believed to regulate their highly organized actin cytoskeleton, is highly expressed. Since the unique structure of podocytes renders them particularly susceptible to changes in the actin cytoskeleton, $\alpha$-actinin-4 mutations can have drastic consequences for the kidney. To date, five disease-causing point mutations in the actin binding domain of $\alpha$-actinin-4 have been identified [24]. All of these mutations increase the protein's actin binding affinity, and lead to abnormal actin aggregation and foot process effacement.

One particular point mutation, which encodes a K255E amino acid exchange in the $\alpha$-actinin-4 protein and is known to cause FSGS and kidney failure in humans, has been extensively investigated by Weins *et al.* [25]. A mouse model homozygous for the mutation exhibits large actin/$\alpha$-actinin-4 aggregates in the podocytes, and subsequently develops a form of collapsing glomerulopathy. In standard cosedimentation assays of actin and $\alpha$-actinin-4 , the equilibrium dissociation constant for the mutant has been determined to be $K_{\mathrm{d,mut}} = 0.046\,\mu\mathrm{M}$, almost six times lower than that of the wild-type, $K_{\mathrm{d,wt}} = 0.267\,\mu\mathrm{M}$. Further, the mutant saturates actin at one dimer per two actin monomers, whereas the wild-type saturates at one dimer per four actin monomers. Weins *et al.* attribute these differences to a conformational change in the protein. Each $\alpha$-actinin monomer is composed of an N-terminal F-actin binding domain, four spectrin repeats, and a C-terminal $Ca^{2+}$ binding domain. In wild-type $\alpha$-actinin-4, the actin binding domain contains two actin binding sites, and its actin affinity can be regulated by $Ca^{2+}$ binding to the neighboring N-terminal domain of the second $\alpha$-actinin-4 monomer. An additional actin binding site is partially buried in the "closed" conformation of the wild-type. The K255E mutation is believed to lead to a higher propensity of the open conformation, which exposes the otherwise buried actin binding site. The mutant has also been shown to be insensitive to regulation by $Ca^{2+}$. This explanation is

corroborated by the fact that inactivation of the additional binding site returns the affinity of the mutant to that of the wild-type, while leaving the affinity of the wild-type unaltered. Weins *et al.* propose that the different stoichiometric ratios of $\alpha$-actinin-4 to actin can be ascribed to greater geometric flexibility of the mutant, which allows it to access every binding site along an actin filament. This flexibility also serves to explain their observation that actin polymerized in the presence of mutant $\alpha$-actinin-4 forms networks of thin actin bundles, whereas the wild-type tends to connect actin into thicker, parallel bundles. Using miniature falling ball viscometry, Weins *et al.* have found that the mutant results in an abrupt viscosity increase, signifying the gel point of the network, at a much lower cross-linker concentration than the wild-type [25]. Further comparative investigations of the viscosity and elasticity of networks with wild-type and mutant $\alpha$-actinin-4 can provide more insight into the disease mediating characteristics of the mutant, especially in view of the pivotal role of the actin cytoskeleton for podocytes; however, systematic studies of actin networks cross-linked specifically with $\alpha$-actinin-4 have not been performed previously.

This thesis provides a detailed analysis, based on rheological data, of the viscoelastic properties of in vitro networks formed from actin with wild-type and K255E-mutant $\alpha$-actinin-4. The difference between the two cross-linkers is most apparent in measurements of the elastic and viscous moduli as a function of the frequency of the applied oscillatory shear stress (section 3.2). The effect of different binding affinities on the macroscopic network dynamics is contrasted with the effect of varied cross-linker concentration (section 3.3) and temperature (section 3.4).

# Chapter 2

# Materials and Methods

## 2.1 Materials

Actin was provided by Fumihiko Nakamura and Thomas Stossel (Brigham and Women's Hospital, Harvard Medical School), who prepared it from rabbit skeletal muscle in a polymerization-depolymerization cycle, and subsequently further purified it by gel filtration. G-actin was stored in G-buffer (2 mM Tris-HCl, pH 7.4, 0.5 mM ATP, 0.5 mM 2-Mercaptoethanol, 0.2 mM $CaCl_2$) at -80 °C. Wild-type and mutant $\alpha$-actinin-4 were provided by Astrid Weins and Martin Pollak (Brigham and Women's Hospital, Harvard Medical School). Baculovirus-expressed recombinant wild-type and K255E mutant $\alpha$-actinin-4 was generated from human cDNA sequences by ProteinOne (College Park, MD, USA) [25] and stored in $\alpha$-actinin buffer (20 mM Tris-HCl, pH 7.9, 20% Glycerol, 100 mM NaCl, 1 mM DTT, 0.2 mM EDTA) at -80 °C.

## 2.2 Network formation

Networks of various cross-linker concentrations were formed by mixing 23.8 $\mu$M (1 mg/ml) G-actin solution with $\alpha$-actinin-4 solutions of concentrations ranging from 0.03 $\mu$M to 1.9 $\mu$M, corresponding to molar ratios of $\alpha$-actinin-4 to actin, $R$, between $R = 0.00125$ and $R = 0.08$. Polymerization was initiated by addition of 5x polymerization buffer (50 mM Tris-HCl,

pH 7.4, 500 mM KCl, 5 mM MgCl, 2.5 mM EGTA, 2.5 mM ATP). The samples were then immediately transferred to the rheometer or confocal microscope, respectively.

## 2.3 Network visualization

Actin was fluorescently stained with 2 $\mu$M Alexa Fluor 488 phalloidin (Invitrogen). Samples of 10 $\mu$l in volume were confined between two glass cover slips spaced at $\sim$1 mm, and examined under a Zeiss LSM 510-Meta confocal microscope with a 63x objective. Fluorescence was excited with an Argon laser at 488 nm, and the signal was filtered by a 505 nm long pass filter.

## 2.4 Bulk rheology

Oscillatory measurements of the elastic modulus $G'$ and the viscous modulus $G''$ were performed with a controlled stress AR-G2 rheometer (TA Instruments). The sample was loaded into a cone-plate geometry with a diameter of 20 mm, a cone angle of 2°, and a gap size of 50 $\mu$m; the sample volume was 70 $\mu$l. A solvent trap was used to prevent drying. Immediately following sample transfer to the rheometer, polymerization was monitored for a period of one to two hours through point measurements of the viscoelastic moduli in five minute intervals at a strain of 0.5% and an oscillation frequency of 0.1 Hz. The frequency dependence of the linear viscoelastic moduli $G'$ and $G''$ was determined between 0.01 Hz and 10 Hz. To ensure that data was taken in the linear regime, where the network response is proportional to the amplitude of the imposed oscillatory stress, the instrument was operated in its strain-controlled mode at strains between 0.5% and 2%, depending on the strength of the network. For each measurement of the frequency dependence, the temperature was held constant, if not stated otherwise, at 25 °C. To investigate the temperature dependence of the network dynamics, the temperatures for different measurements at the same sample were varied between 5 °C and 40 °C by means of the Peltier temperature control of the lower rheometer plate.

# Chapter 3

# Comparison of the structures and viscoelastic properties of actin networks cross-linked with wild-type and mutant $\alpha$-actinin-4

## 3.1 Network structures

Actin polymerized in vitro forms finely meshed, homogeneous, isotropic three-dimensional networks (Fig. 3-1(a)). The addition of cross-linking proteins often results in networks of larger mesh size, which consist of actin bundles comprising many individual filaments. We confirmed by confocal fluorescence microscopy that this general trend also holds for networks of actin with wild-type and mutant $\alpha$-actinin-4 , prepared in the same way as the samples used for our rheological measurements. At a concentration of one $\alpha$-actinin-4 molecule per hundred actin monomers, $R = 0.01$, the wild-type cross-linker (Fig. 3-1(b)) appears to form a coarser network than the mutant (Fig. 3-1(c)), consistent with the larger bundle diameter reported by Weins *et al.* for actin cross-linked with wild-type $\alpha$-actinin-4. However, we find the cross-linked networks interspersed with large actin agglomerates (Figs. 3-1(b) and

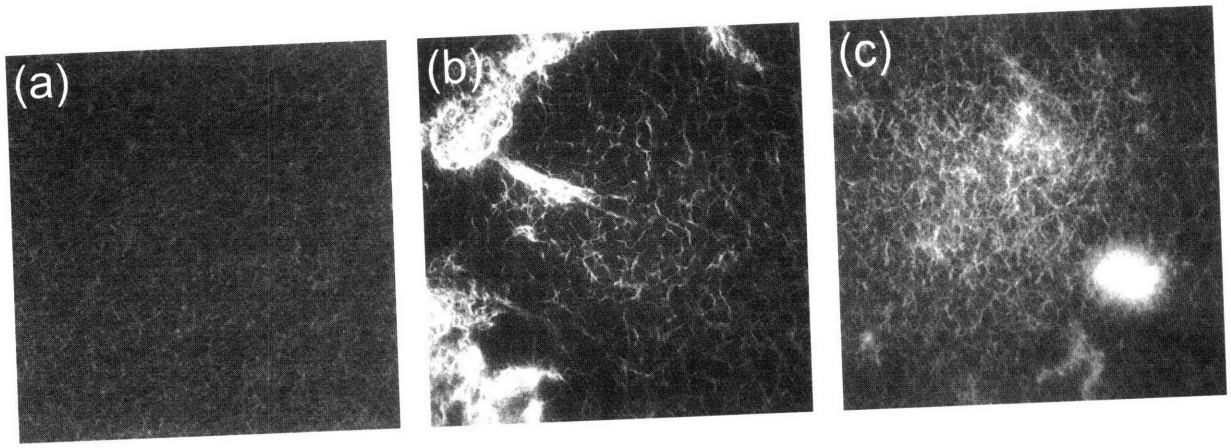


Figure 3-1: Confocal images of networks formed of actin (1 mg/ml) (a) without cross-linker, (b) with wild-type $\alpha$-actinin-4 ($R = 0.01$), and (c) with mutant $\alpha$-actinin-4 ($R = 0.01$). Actin is fluorescently labeled with Alexa-Flour-Phalloidin (excitation at 488 nm). Image size: 153.6 $\mu$m x 153.6 $\mu$m.

(c)), whose size and number vary from sample to sample, and tend to increase with higher cross-linker concentration. Moreover, the homogeneous network regions vary in mesh size even within one sample, thus rendering a quantitative comparison of the effects of wild-type and mutant on the network structure unfeasible.

## 3.2 Overview over the frequency-dependent viscoelasticity of the networks

In spite of the large sample-to-sample variations of the network structures and inhomogeneities at length scales of tens of micrometers, the cross-linked networks exhibit robust rheological properties–a consequence of sample averaging over larger dimensions. At a molar ratio of $R = 0.01$, cross-linking increases the network stiffness by about an order of magnitude. The elastic and viscous moduli vary greatly with the frequency of the applied oscillatory shear stress. At the intermediate frequencies which we can access through bulk rheological measurements, the linear viscoelasticity is characterized by a nearly frequency-independent plateau in the elastic modulus $G'$, and a corresponding minimum of the viscous

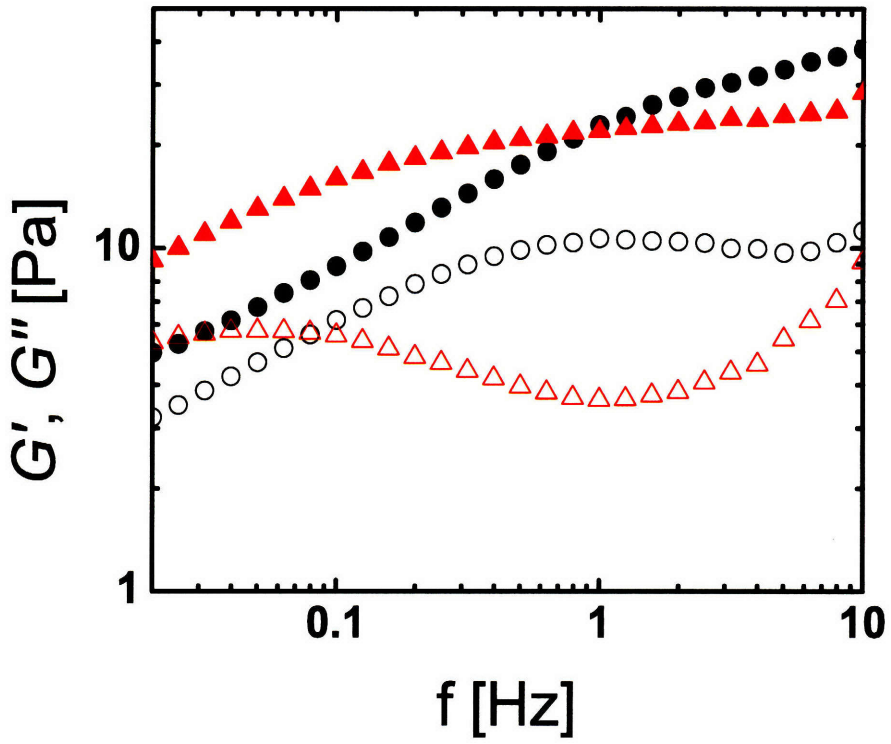


Figure 3-2: Frequency dependence of the elastic modulus $G'$ (solid symbols) and the viscous modulus $G''$ (open symbols) of actin networks with wild-type (black circles) and mutant (red triangles) $\alpha$-actinin-4 at a molar ratio of $\alpha$-actinin-4 to actin of $R = 0.01$. The networks are characterized by an elastic plateau, and a relaxation towards fluid properties at lower frequencies. The response for mutant $\alpha$-actinin-4 appears shifted towards lower frequencies, and exhibits a higher ratio $G'/G''$ at the plateau frequency.

modulus $G''$ (3-2). A direct comparison of the effect of wild-type (black circles) and mutant (red triangles) cross-linker reveals that the latter results in a more distinct elastic plateau. Moreover, the characteristic frequency of the plateau, $f_{\text{plateau}}$, which we define as the frequency at which $G''$ assumes its local minimum, is smaller for the mutant than for the wild-type.

In the high frequency limit, we expect the network viscoelasticity to be dominated by the thermal bending fluctuations of individual filaments, leading to an increase of both moduli with frequency with a power of 3/4 [16, 8]. We cannot measure at frequencies high enough to confirm this dependence, but we observe for several samples the onset of an ascent of $G'$ and $G''$ with an increasing slope of up to 0.6 in a log-log plot.

At low frequencies, the networks carry the signature of a structural relaxation process: The viscous modulus $G''$ approaches the elastic modulus with decreasing frequency, passing through a maximum value and then decreasing along with $G'$. We expect $G''$ to eventually exceed $G'$, indicating a relaxation of the network behavior to fluid properties. While for most data sets, the range of our measurements does not extend to low enough frequencies to verify this cross-over, we do observe it in a few cases. For comparisons of relaxation frequencies across samples, we take $f_{\text{relax}}$ to be the well-defined frequency at which $G''$ reaches a local maximum (3-2). In comparing networks with wild-type and mutant $\alpha$-actinin-4, we find that $f_{\text{relax}}$ is more than an order of magnitude lower for the mutant. Taken together with the smaller equilibrium dissociation constant of mutant $\alpha$-actinin-4 [25], this observation suggests that the relaxation of the macroscopic network might be related to the microscopic unbinding of the cross-linker. When an $\alpha$-actinin-4 dimer dissociates from actin at either binding site, the cross-link breaks, and filaments can locally slide with respect to each other. The cross-linker may bind again to actin at both ends, thereby reforming a link in the network. If this happens before other cross-linkers in the vicinity of the broken link detach, a macroscopic relaxation of the network is not possible. However, our data suggests that sufficiently many cross-linkers unbind simultaneously to allow the network to structurally relax, and to become fluid-like at low frequencies.

## 3.3 Cross-linker concentration and network strength

We extend our comparison of wild-type and mutant $\alpha$-actinin-4 by investigating the effect of the cross-linker concentration on the frequency dependent viscoelasticity of the networks. With increasing concentration of wild-type or mutant cross-linker, $G'$ and $G''$ rise noticeably over the entire frequency range of our measurements. While the elastic modulus is shifted upwards without a change in its frequency dependence, an increase in concentration does alter the frequency dependence of the viscous modulus. At the plateau, the increase in $G'$ with concentration tends to be greater than that in $G''$. Thus, increasing the $\alpha$-actinin-4 concentration enhances the plateau, pushing the network properties further towards that of a solid, as illustrated with representative network responses for relative $\alpha$-actinin-4 concentrations of $R = 0.005$ (red triangles), 0.01 (black circles), and 0.02 (blue inverted triangles) in Fig. 3-3(a) for the wild-type and in Fig. 3-3(b) for the mutant cross-linker. Interestingly, an increased amount of wild-type $\alpha$-actinin-4 effects the shape of the viscoelasticity in the vicinity of the plateau qualitatively similarly to a replacement of wild-type by mutant cross-linker. In comparing the curves in Figs. 3-3(a) and 3-3(b), we see that the behavior for the wild-type cross-linker of the highest concentration shown resembles that of the mutant with the lowest concentration, albeit shifted along both axes. Based on this observation, we investigate whether the altered properties of the mutant can partly be compensated for by a decreased concentration. We find that this is indeed the case: The frequency dependent viscoelasticity of a network with wild-type $\alpha$-actinin-4 at a high concentration of $R = 0.04$ (black circles) and a network with mutant $\alpha$-actinin-4 at a four times lower concentration ($R = 0.01$, red triangles), shown in 3-4(a), overlap remarkably well if the mutant curve is shifted towards higher frequencies and higher viscoelastic moduli, as illustrated in Fig. 3-4(b). Similarly, the curves for samples with a medium amount of wild-type ($R = 0.01$) and a low amount of mutant ($R = 0.0025$), which are shown in Fig. 3-4(c), can be scaled nearly perfectly (Fig. 3-4(d)). This intriguing scaling behavior might have profound implications for the understanding of $\alpha$-actinin-4 in its effect on the network properties.

In order to test the statistical significance of our qualitative observations, we extract

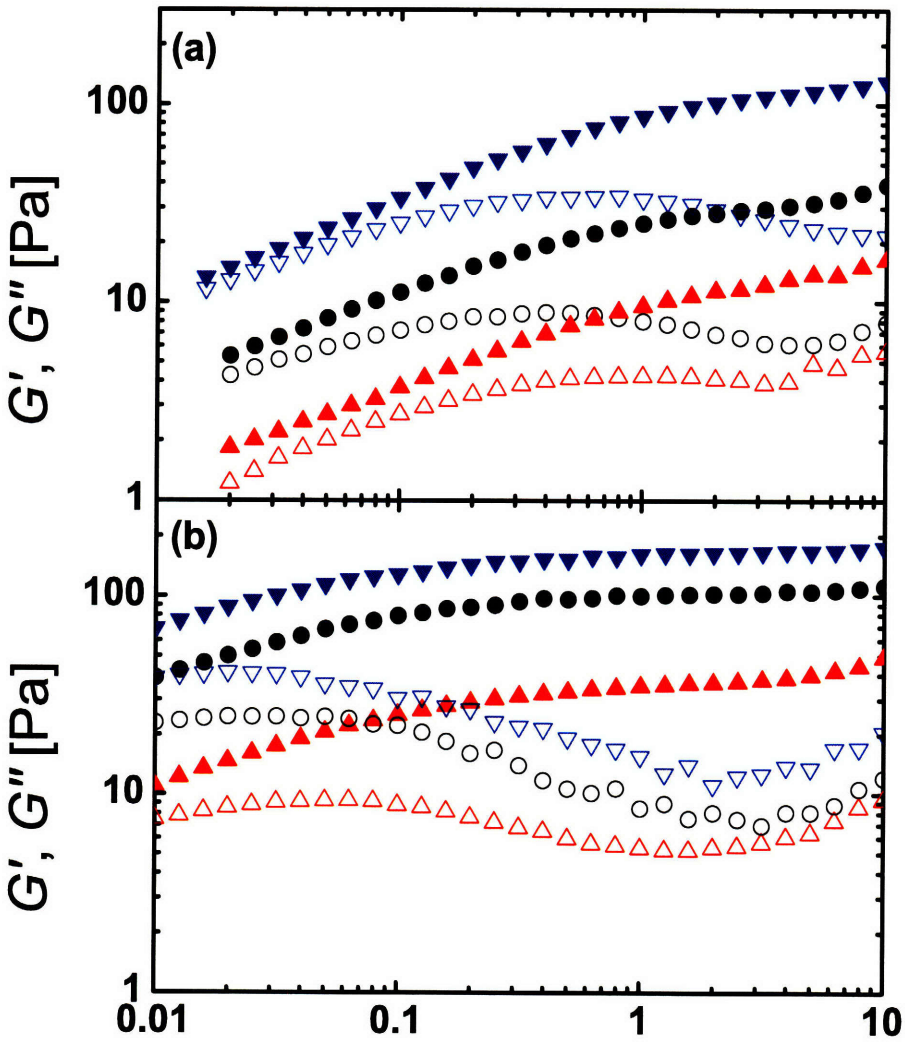


Figure 3-3: Frequency dependence of the elastic modulus $G'$ (solid symbols) and the viscous modulus $G''$ (open symbols) of actin networks with (a) wild-type and (b) mutant $\alpha$-actinin-4 at molar ratios of $\alpha$-actinin-4 to actin of $R = 0.005$ (red triangles), $R = 0.01$ (black circles), and $R = 0.02$ (blue inverted triangles). For both types of cross-linker, the elastic plateau modulus increases with concentration. Moreover, the plateau is more pronounced and appears at higher frequencies for increased concentration.

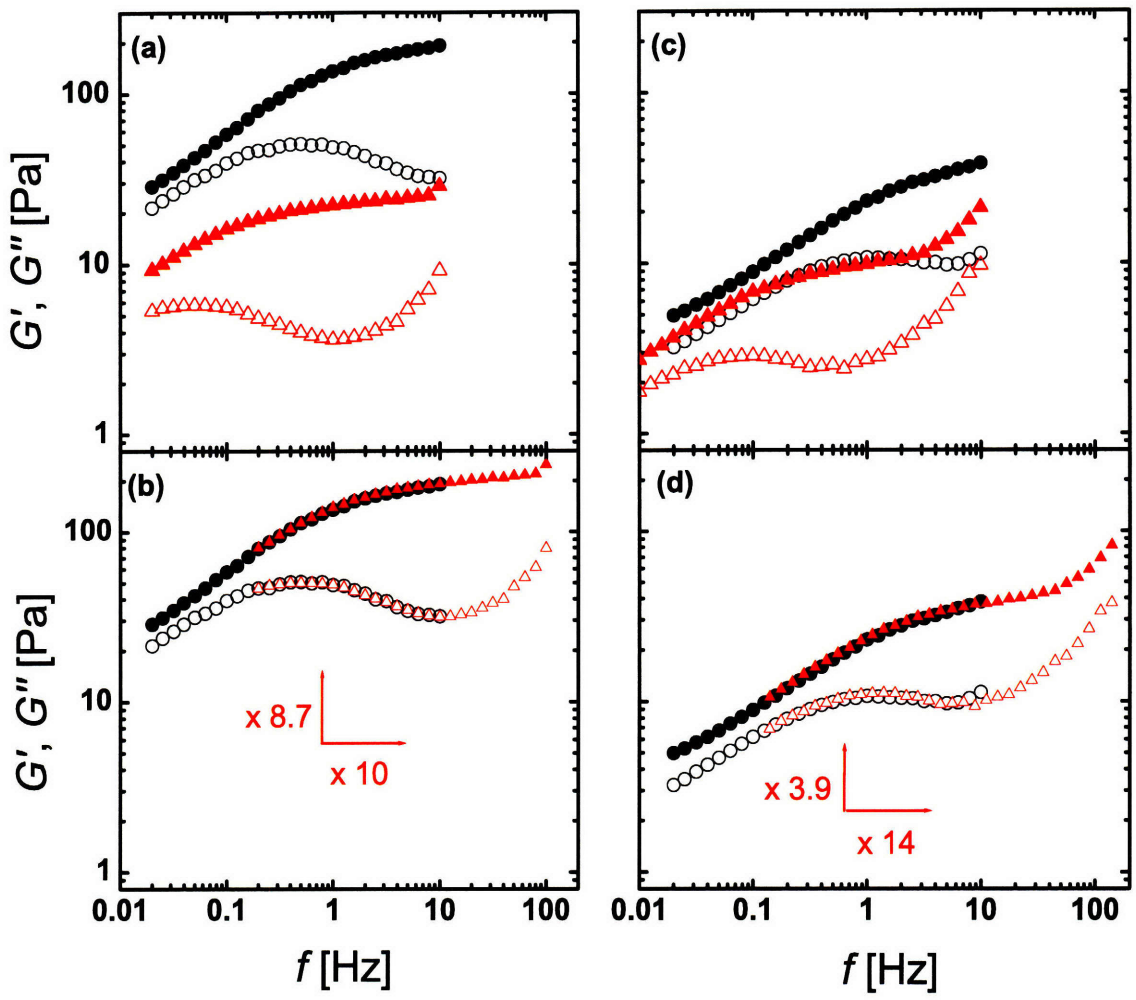


Figure 3-4: The frequency dependence of $G'$ (solid symbols) and $G''$ (open symbols) of actin networks with wild-type (black circles) and mutant (red triangles) $\alpha$-actinin-4 of different concentrations can be scaled onto one curve. For example, samples with wild-type at high concentration ($R = 0.04$) and mutant at medium concentration ($R = 0.01$), as shown in (a), overlap if the mutant is shifted by a factor of 10 in frequency and by a factor of 8.7 in the moduli (b). Similarly, samples with wild-type at medium concentration ($R = 0.01$) and mutant at low concentration ($R = 0.0025$), shown in (c), overlap if the mutant is shifted by a factor of 14 in frequency and by a factor of 3.9 in the moduli (d).

several characteristic quantities from the frequency dependent viscoelasticity of a larger set of samples, comprised of 24 networks with wild-type and 18 with mutant $\alpha$-actinin-4 and containing the samples presented in Figs. 3-3 and 3-4, and plot these quantities as a function of cross-linker concentration. We confirm that the elastic modulus at the plateau frequency, $G'_{\text{plateau}}$, increases with cross-linker concentration for both wild-type (black circles) and mutant (red triangles), as shown in Fig. 3-5(a). Above relative $\alpha$-actinin-4 concentrations of $R = 0.005$, the plateau modulus follows a power law of $G'_{\text{plateau}}\ R^{4/3}$ (solid lines). A similar concentration dependence has previously been observed for other cross-linkers [23, 7]. We infer from Fig. 3-5(a) that the values of $G'_{\text{plateau}}$ for wild-type and mutant $\alpha$-actinin-4 at the same concentration are comparable. This might at first seem surprising; however, if we assume a first order binding reaction between actin and $\alpha$-actinin-4, we calculate that at an actin monomer concentration of 23.8 $\mu$M, almost all cross-linkers are bound to actin. The higher binding affinity of the mutant therefore results only in a marginal increase of bound $\alpha$-actinin-4 from 98.8% to 99.8% of the total cross-linker amount.

While the mutant does not appear to increase the overall network strength, it does render the network more solid-like, as is evident from the consistently higher values for the ratio of $G'$ and $G''$ at the plateau, which is plotted in Fig. 3-5(b). As observed before and confirmed by the larger data set, this ratio increases slightly with concentration. In addition to $G'/G''$ at the plateau frequency, the prominence of the elastic plateau is characterized by the width of the frequency range spanned between $f_{\text{relax}}$ and $f_{\text{plateau}}$. We find that the plateau frequency increases with cross-linker concentration (Fig. 3-5(c)), whereas the relaxation frequency remains approximately constant (Fig. 3-5(d)). As a result, the plateau tends to be the wider, the higher the amount of $\alpha$-actinin-4. Furthermore, networks with the mutant cross-linker exhibit a slightly lower plateau and a significantly lower relaxation frequency. Consequently, the plateau width is greater for the mutant.

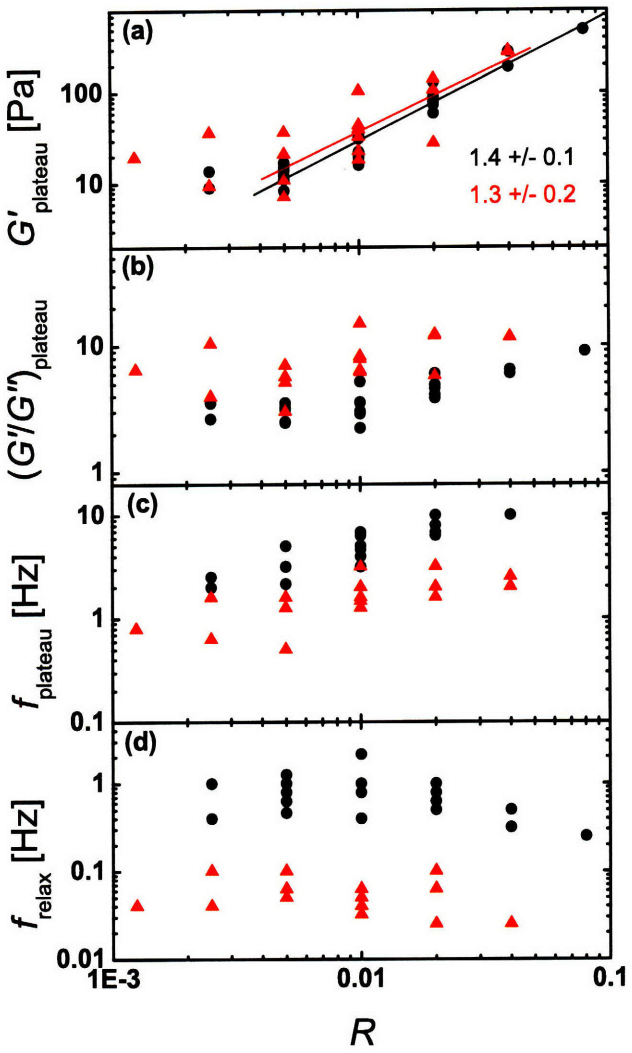


Figure 3-5: Characteristic features of the frequency-dependent viscoelasticity as a function of the relative concentration $R$ of wild-type (black circles) and mutant (red triangles) $\alpha$-actinin-4. (a) The plateau modulus $G'_{\text{plateau}}$ has comparable values for wild-type and mutant, and increases with cross-linker concentration. Above $R = 0.005$, the plateau modulus follows a power law for both cross-linker types, as indicated by the solid lines for wild-type (black) and mutant (red) and their respective slopes (lower right). (b) The ratio of the plateau modulus and the corresponding viscous modulus, $(G'/G'')_{\text{plateau}}$, grows weakly with increasing cross-linker concentration, and is on average higher for the mutant than for the wild-type at the same concentration. (c) The frequency at which the elastic plateau occurs (minimum in $G''$) increases weakly with cross-linker concentration, and is systematically smaller for the mutant. (d) The relaxation frequency of the network (maximum in $G''$) appears to be independent of the cross-linker concentration, and is about an order of magnitude smaller for the mutant.

## 3.4 Temperature and network dynamics

The networks with mutant $\alpha$-actinin-4 differ most significantly from their wild-type counterparts in that their relaxation frequencies are consistently lower by at least an order of magnitude for concentrations ranging from $R = 0.0025$ to $R = 0.04$ (Fig. 3-5(d)). We propose that this shift in time scales is a consequence of a smaller actin/$\alpha$-actinin-4 unbinding rate for the mutant. Since the equilibrium dissociation constant $K_\mathrm{d}$ is the ratio of the dissociation rate, or off-rate $k_-$, and the association rate, or on-rate $k_+$, we cannot say with certainty which of the rates differs between wild-type and mutant. However, Weins *et al.* [25], following an argument of Wachsstock *et al.* [21], have explained their observation of a stronger tendency of wild-type $\alpha$-actinin-4 to bundle actin partly by assuming a higher dissociation rate for the wild-type, consistent with the higher value they determined for $K_\mathrm{d}$. If we adopt this assumption, the dissociation rate of the mutant follows to be about six times smaller than that of the wild-type. Given that our practical definition of $f_\mathrm{relax}$ as the frequency at which $G''$ reaches a local maximum only approximates the frequency at which the relaxation actually occurs, this factor is consistent with the observed factor of slightly more than 10 between the relaxation frequencies of wild-type and mutant cross-linked networks (Figs. 3-2, 3-3, and 3-5(d)).

The proposed direct relationship between the characteristic relaxation frequency of the macroscopic network and the microscopic dissociation rates of its constituents is intriguing. By controlling the dissociation rates, we can test whether the collective network relaxation is indeed related to the unbinding of cross-linkers. If we assume that the dissociation rate is limited by the fraction of cross-linkers with sufficient kinetic energies to overcome the activation energy barrier of the reaction, an obvious way to influence this rate is by means of the temperature. Based on our proposition, we expect that the characteristic frequencies of the networks increase with increasing temperature. Our measurements of the dynamic viscoelastic response of cross-linked networks for different temperatures verify this dependence, as demonstrated in Fig. 3-6 for networks with cross-linker concentrations of $R = 0.01$ at 15 °C (blue inverted triangles), 25 °C (black circles), and 35 °C (red triangles). Since the relaxation

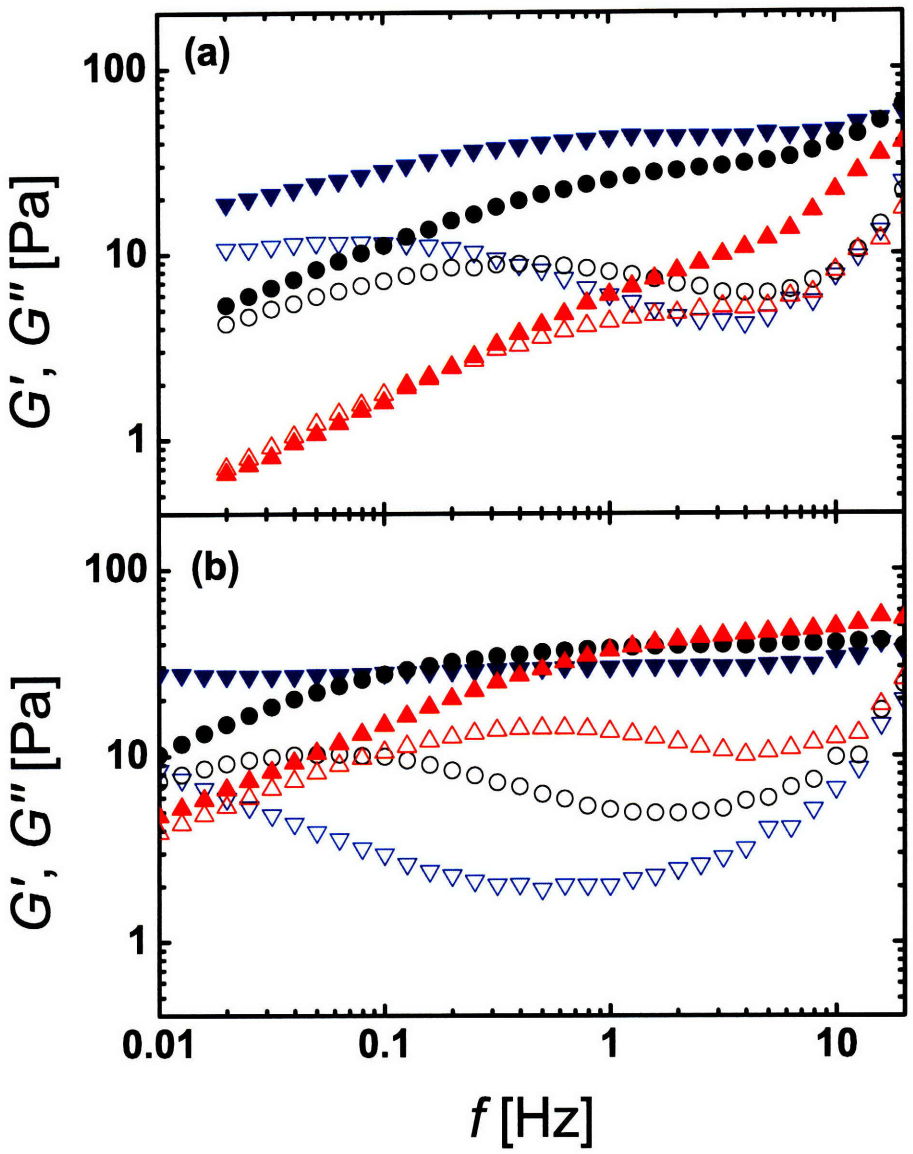


Figure 3-6: Frequency dependence of the elastic modulus $G'$ (solid symbols) and the viscous modulus $G''$ (open symbols) of actin networks with (a) wild-type and (b) mutant $\alpha$-actinin-4 (molar ratio of $\alpha$-actinin-4 to actin $R = 0.01$) at 37 °C (red triangles), 25 °C (black circles), and 15 °C (blue inverted triangles). Similarly to a high cross-linker concentration, a lower temperature results in a more pronounced elastic plateau. In addition, a temperature decrease shifts the network relaxation towards lower frequencies.

frequency ($f_{\text{relax}}$) rises faster with temperature than the plateau frequency ($f_{\text{plateau}}$), the elastic plateau spans a wider frequency range at lower temperatures. Moreover, a decrease in temperature–similarly to an increase in $\alpha$-actinin-4 concentration–increases the ratio of $G'$ to $G''$ at the plateau, rendering the network more solid-like. In contrast to a change in cross-linker concentration,which influences the prominence of the elastic plateau while leaving the relaxation frequency of the network unaltered, a change in temperature appears to influence both network features. We expect the effect of the mutation to be largely compensated for by an appropriate temperature increase, such that the viscoelasticity curves of networks with wild-type and mutant $\alpha$-actinin-4 at different temperatures coincide without significant scaling in frequency or moduli. Our observations confirm this notion. For example, we find that the viscoelasticity of the network with wild-type $\alpha$-actinin-4 at 25 ° shown in 3-6(a) (black circles) agrees well with that of the network with mutant cross-linker at 37 ° shown in 3-6(b) (red triangles); a direct comparison is provided in 3-7(a). Similarly, the viscoelastic responses of networks with wild-type (black circles) and mutant (red triangles) $\alpha$-actinin-4 at $R = 0.02$ and temperatures of 15 °C and 32.5 °C nearly coincide, as illustrated in 3-7(b).

To analyze the temperature dependence of the relaxation frequency more quantitatively, we measure the frequency dependent viscoelasticity at temperatures between 5 °C and 40 °C for six samples of each cross-linker type with relative cross-linker concentrations ranging from $R = 0.00125$ to $R = 0.08$, and extract $f_{\text{relax}}$ from these curves. For a few samples, the relaxation frequency falls outside the range of our measurements (0.01 Hz–10 Hz) at the lowest temperatures (e.g. blue curve in Fig. 3-6(b)), and the corresponding data are not included in our compilation. We assume that the temperature dependence of the dissociation rates of wild-type and mutant $\alpha$-actinin-4 follows the Arrhenius equation:

$$k_{-} = k_0 \cdot \exp^{-E_{\text{a}}/(k_{\text{B}}\, N_{\text{A}}\, T)} \tag{3.1}$$

Herein, $E_{\text{a}}$ denotes the molar activation energy which needs to be overcome for the dissociation reaction to take place, and $k_0$ describes the rate at which unbinding is attempted; $k_{\text{B}}$ and $N_{\text{A}}$ are the Boltzmann and Avogadro constants, respectively. In order to test whether

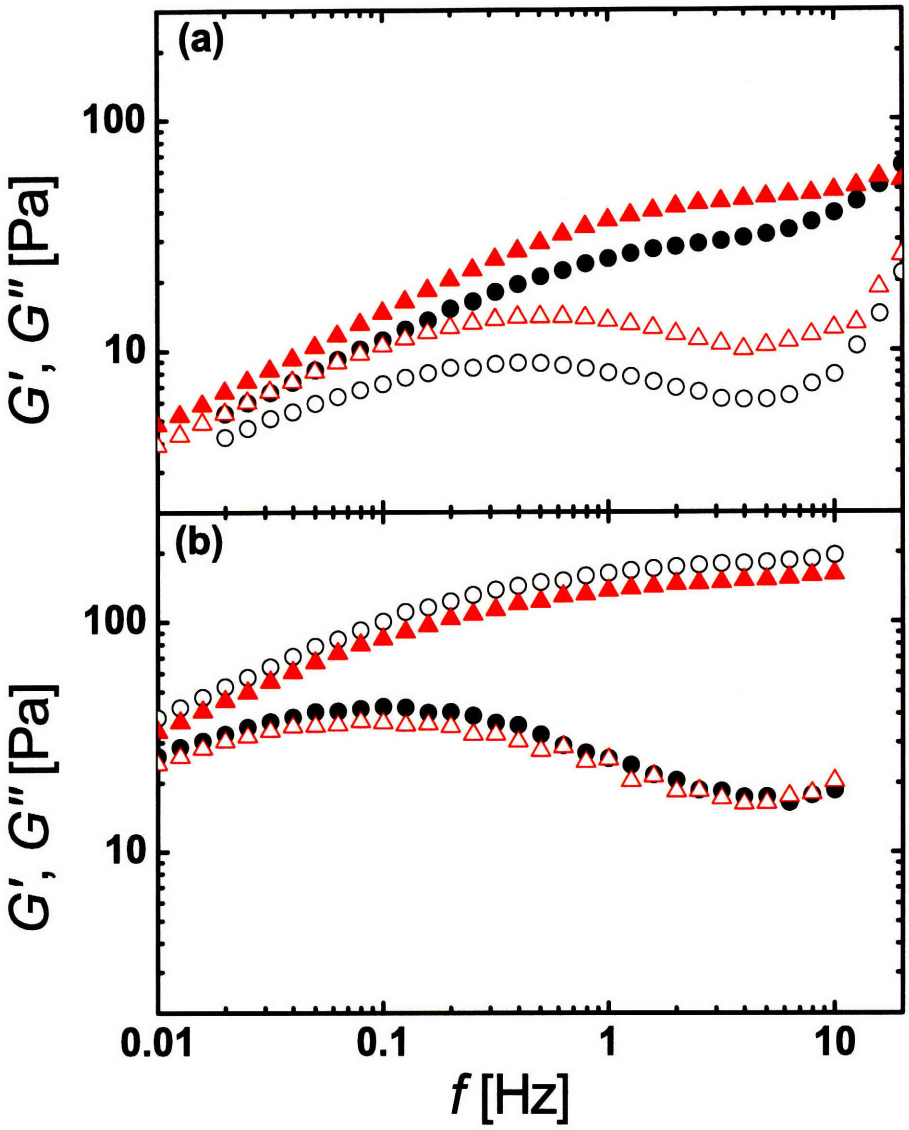


Figure 3-7: An increase in temperature can return the viscoelasticity of networks with mutant $\alpha$-actinin-4 (red triangles) to that of networks with wild-type cross-linker (black circles), as illustrated by the frequency dependence of $G'$ (solid symbols) and $G''$ (open symbols) for (a) $R = 0.01$, wild-type at 25 °C, mutant at 37 °C, and (b) $R = 0.02$, wild-type at 15 °C, mutant at 32.5 °C. In contrast to the scaling behavior for mutant and wild-type at different concentrations, a shift in frequency or moduli is not necessary.

the macroscopic relaxation frequencies of the networks exhibit the same temperature dependence, we plot $f_{\text{relax}}$ on a natural-logarithmic scale over the inverse of the thermal energy $k_{\text{B}}\,N_{\text{A}}\,T$, measured in Kilojoules per mole. The relaxation frequencies for wild-type (black circles) and mutant (red triangles) $\alpha$-actinin-4 form two distinct bands of data points, separated by about an order of magnitude, as shown in Fig. 3-8. The width of these bands can be attributed to the various cross-linker concentrations in the samples. However, since the concentration dependence of the relaxation frequency is very weak, we do not distinguish between different concentrations in our plot. The temperature dependent relaxation frequencies of wild-type and mutant can indeed be described by the Arrhenius equation, as indicated by straight line fits with slopes of (119.24.4) kJ/mol for the wild-type (black) and (126.28.0) kJ/mol for the mutant (red). These values are on the order of typical protein interaction energies, allowing us to identify them with the activation energies of the microscopic dissociation rates.

The disparity in equilibrium dissociation constants $K_{\text{d}}$ between wild-type and mutant $\alpha$-actinin-4 can plausibly be accounted for by a difference in the activation energies. As Weins *et al.* have established, the binding surface of the mutant cross-linker is extended by a third binding site, which is buried in the wild-type. This additional site could simply decrease the energy level of the bound state, and thus increase the energy barrier $E_{\text{a}}$ for unbinding. Since the activation energy appears in the exponential, a small difference $E_{\text{a,mut}} - E_{\text{a,wt}}$ of 4.5 kJ/mol suffices to cause a six times lower dissociation rate $k_{\text{-,mut}}$ consistent with the lower equilibrium dissociation constant observed for the mutant [25]. This difference in activation energies is consistent with our data.

An alternative explanation lies in sequential binding of the two sites that the mutant $\alpha$-actinin-4 has in common with the wild-type, and its additional binding site, as described by the following chemical reaction:

$$\alpha + \text{Act} \rightleftharpoons (\alpha - \text{Act}) \rightleftharpoons (\alpha - \text{Act})^{*} \tag{3.2}$$

We assume that the first reaction, including its association and dissociation rates, is identical

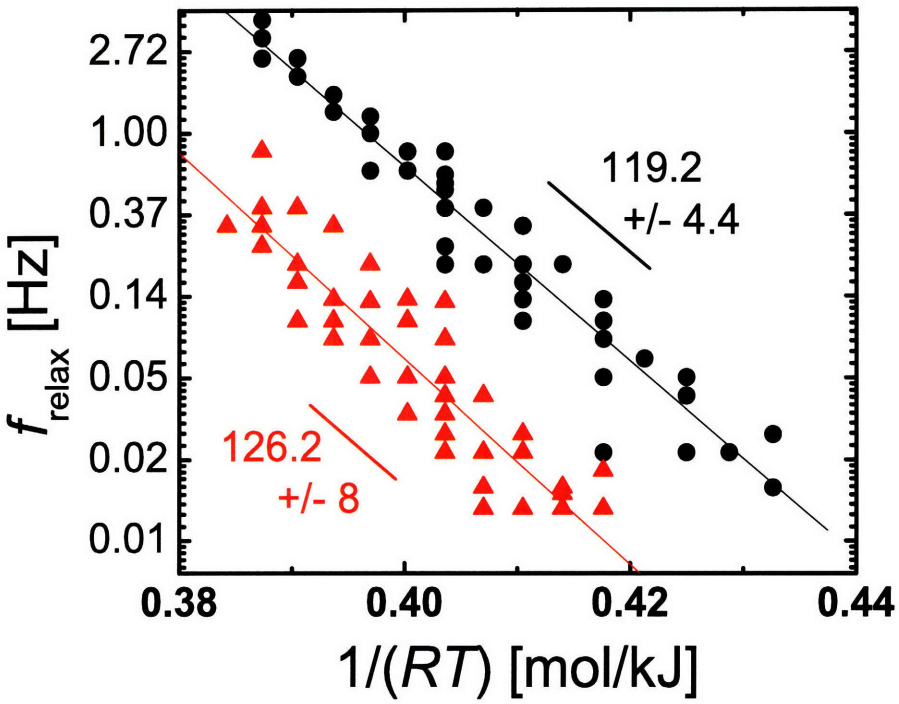


Figure 3-8: Temperature dependence of the network relaxation frequency. The logarithm of the frequency is plotted as a function of the inverse thermal energy. For both wild-type (black circles) and mutant (red triangles) cross-linker, the relaxation frequency follows the Arrhenius equation. The slopes, which correspond to an activation energy barrier in the Arrhenius equation, are comparable. Relaxation frequencies for the mutant are consistently lower by about an order of magnitude.

for wild-type and mutant. The second reaction only applies to the mutant, and describes its binding to actin at the third binding site, which results in a distinct, energetically favorable bound state. The overall concentration of mutant cross-linker, $[\alpha]_{\mathrm{tot}}$, is in this case:

$$\begin{aligned}[\alpha]_{\mathrm{tot}} &= [\alpha]_{\mathrm{free}} + [\alpha - \mathrm{Act}] + [\alpha - \mathrm{Act}^*] = [\alpha]_{\mathrm{free}} + [\alpha - \mathrm{Act}] \cdot \left(1 + \frac{k_+^*}{k_-^*}\right) \\ &= [\alpha]_{\mathrm{free}} \cdot \left(1 + \frac{k_+}{k_-} \cdot [\mathrm{Act}] \cdot \left(1 + \frac{k_+^*}{k_-^*}\right)\right)\end{aligned} \tag{3.3}$$

The dissociation constant $K_{\mathrm{d,mut}}$, as measured in a cosedimentation assay from the amount of free and bound cross-linker, can be calculated from the dissociation constant for the wild-type and the reaction rates for the second binding step:

$$K_{\mathrm{d,mut}} = \frac{[\alpha]_{\mathrm{free}}\,[\mathrm{Act}]}{[\alpha]_{\mathrm{tot}} - [\alpha]_{\mathrm{free}}} = \frac{[\mathrm{Act}]}{\frac{1}{K_{\mathrm{d,wt}}} \cdot [\mathrm{Act}] \cdot \left(1 + \frac{k_+^*}{k_-^*}\right)} = \frac{K_{\mathrm{d,wt}}}{1 + \frac{k_+^*}{k_-^*}} \tag{3.4}$$

In order to recover the experimentally determined factor of six between the binding affinities of mutant and wild-type, we need to assume a ratio $k_+^*/k_-^* = 5$. This ratio also implies that most of the mutant is bound to actin at all three binding sites, and only one sixth is in the weaker bound state. We can now explain the lower relaxation frequency of networks with mutant $\alpha$-actinin-4 by relating it to the number of cross-linkers that unbind per unit time, which is the product of $k_-$, the rate at which weakly bound mutant $\alpha$-actinin-4 dissociates completely from actin, and the number of mutant in this weaker binding state. With this interpretation, the shift in relaxation frequencies between wild-type and mutant stems from a lower prefactor for the mutant, which reflects the smaller fraction of cross-linker available for unbinding and is only weakly temperature dependent. The main temperature dependence of the relaxation frequency is determined by the exponential in $k_-$, which is the same for wild-type and mutant. Consequently, the slope of the natural logarithm of $f_{\mathrm{relax}}$ over $1/k_{\mathrm{B}}\,N_{\mathrm{A}}\,T$, which is given by the corresponding activation energy $E_{\mathrm{a}}$, is the same for both types of cross-linker as well. Our measurements of the temperature dependent macroscopic relaxation frequencies of networks with wild-type and mutant do not provide a criterion by which to

choose one of the proposed explanations over the other. Both are consistent with our data, and support the suggested relationship between the network dynamics and the microscopic binding dynamics.

# Chapter 4

# Conclusion

We have established through rheological measurements that the dynamic viscoelasticity of actin networks formed in vitro in the presence of the cross-linking protein $\alpha$-actinin-4 is characterized by an elastic plateau in the frequency range between 0.1 Hz and 10 Hz, and a relaxation towards fluid properties at lower frequencies. These features result from a combination of the properties of individual actin filaments and the cross-linker dynamics. The high network elasticity at the plateau is a direct consequence of cross-linking, as evidenced by the increased elastic plateau modulus and greater prominence of the plateau at higher cross-linker concentration.

In contrasting the effects of the wild-type cross-linker and a mutant known to have a significantly higher actin binding affinity, we have found the network dynamics for the mutant to be shifted to longer time scales. In particular, networks with mutant $\alpha$-actinin-4 undergo their relaxation at lower frequencies. We explain this phenomenon by proposing that the relaxation of the network on the macroscopic level results from the dissociation of $\alpha$-actinin-4 from actin, which we assume to take place at a lower rate for the mutant, consistent with its smaller equilibrium dissociation constant. In strong support of this explanation, we have shown that the temperature dependence of the network relaxation frequency follows the Arrhenius equation for rate constants of chemical reactions, and allows us to extract a conceivable value of the energy implied in the dissociation reaction. Based on knowledge

about an additional actin binding site exposed in the mutant cross-linker, we suggest two different binding mechanisms: one-step binding with a lower energy level in the bound state for the mutant, and sequential two-step binding, which implies the same temperature dependence, but different prefactors for the dissociation of wild-type and mutant $\alpha$-actinin-4 from actin.

In addition to shifting the relaxation to lower frequencies, the substitution of wild-type by mutant $\alpha$-actinin-4 and a decrease in temperature both result in a more pronounced elastic plateau, thus rendering the network more solid-like. In fact, a higher temperature appears to compensate for the effect of the mutation. An increase in cross-linker concentration likewise alters the frequency dependent viscoelasticity, up to scaling factors in frequency in modulus, in a manner remarkably similar to the change from wild-type to mutant. Whether this apparent scalability has a profound reason that could provide further insight into the properties of cross-linked networks remains a question for future investigations.

Our comparison of actin networks cross-linked with mutant and wild-type $\alpha$-actinin-4 is not the first study of the effect of different binding affinities of actin cross-linkers on the dynamic rheological behavior of the resulting networks. Previous comparative studies have been performed, for example, by Wachsstock *et al.* [22], who have related the different cross-linker dynamics of Acanthamoeba and chicken smooth muscle $\alpha$-actinin to the mechanical properties of the networks. However, the difference between the two cross-linking proteins studied here is unique in that it results from the smallest possible variation in the underlying genetic code–a point mutation. Interestingly, we have found this mutation to have a drastic effect on the properties of in vitro networks at shear frequencies around 1 Hz, close to the human heart rate. In vivo, the pathological consequences of the mutant cross-linker are most apparent in podocytes, which are subject to substantial shear stresses resulting from dynamic capillary pressure. The combination of these facts strongly suggests that altered viscoelastic properties of cross-linked actin networks contribute to the phenotypic changes in diseased kidneys.

# Bibliography


[1] B. Alberts, A. Johnson, J. Lewis, M. Raff, K. Roberts, and P. Walter. *Molecular Biology of the Cell.* Garland Science, New York, 4th edition, 1994.

[2] J. R. Bartles. Parallel Actin Bundles and their Multiple Actin-Bundling Proteins. *Current Opinions in Cell Biology*, 12:72–78, 2000.

[3] P. Cortes, X. Zhao, B. L. Riser, and R. G. Narins. Regulation of Glomerular Volume in Normal and Partially Nephrectomized Rats. *American Journal of Physiology*, 270:F356–F370, 1996.

[4] M. L. Gardel. *Elasticity of F-Actin Networks.* PhD thesis, Harvard University, 2004.

[5] M. L. Gardel, F. Nakamura, J. H. Hartwig, J. C. Crocker, T. P. Stossel, and D. A. Weitz. Prestressed F-Actin Networks Cross-Linked by Hinged Filamins Replicate Mechanical Properties in Cells. *Proceedings of the National Academy of Sciences of the United States of America*, 103(6):1762–1767, 2006.

[6] M. L. Gardel, F. Nakamura, J. H. Hartwig, J. C. Crocker, T. P. Stossel, and D. A. Weitz. Stress-Dependent Elasticity of Composite Actin Networks as a Model for Cell Behavior. *Physical Review Letters*, 96:088102, 2006.

[7] M. L. Gardel, J. H. Shin, F. C. MacKintosh, L. Mahadevan, P. Matsudaira, and D. A. Weitz. Elastic Behavior of Cross-Linked and Bundled Actin Networks. *Science*, 304:1301–1305, 2004.

[8] F. Gittes and F. C. MacKintosh. Dynamic Shear Modulus of a Semiflexible Polymer Network. *Physical Review E*, 58(2):R1241–R1244, 1998.

[9] P. A. Janmey, S. Hvidt, J. Käs, D. Lerche, A. Maggs, E. Sackmann, M. Schliwa, and T. P. Stossel. The Mechanical Properties of Actin Gels–Elastic Modulus and Filament Motions. *Journal of Biological Chemistry*, 269(51):32503–32513, 1994.

[10] J. M. Kaplan, S. H. Kim, K. N. North, H. Rennke, L. A. Correia, H.-Q. Tong, B. J. Mathis, J.-C. Rodrigues-Pérez, P. G. Allen, A. H. Beggs, and M. R. Pollak. Mutations in ACTN4, encoding $\alpha$-Actinin-4, Causes Familial Focal Segmental Glomerulosclerosis. *Nature Genetics*, 24:251–256, 2000.

[11] K. E. Kasza, A. C Rowat, J. Liu, T. E. Angelini, C. P Brangwynne, G. H. Koenderink, and D. A. Weitz. The Cell as a Material. *Current Opinions in Cell Biology*, 19:101–107, 2007.

[12] C. H. Kos, T. C. Le, S. Sinha, J. M. Henderson, S. H. Kim, H. Sugimoto, R. Kalluri, R. E. Gerszten, and M. R. Pollak. Mice Deficient in $\alpha$-Actinin-4 have Severe Glomerular Disease. *The Journal of Clinical Investigations*, 111(11):1683–1690, 2003.

[13] C. A. Krakower, B. K. Nicholes, and S. A. Greenspon. Proteinuria and the Fragility of Normal and Diseased Glomerular Basement Membrane. *Proceedings of the Society for Experimental Biology and Medicine*, 159:324–334, 1978.

[14] R. G. Larson. *The Structure and Rheology of Complex Fluids.* Oxford University Press, New York & Oxford, 1999.

[15] J.-L. Michaud, L. I. Lemieux, M. Dubé, B. C. Vanderhyden, S. J. Robertson, and C. R. J. Kennedy. Focal and Segmental Glomerulosclerosis in Mice with Podocyte-Specific Expression of Mutant $\alpha$-Actinin-4. *Journal of the American Society of Nephrology*, 14:1200–1211, 2003.

[16] D. C. Morse. Viscoelasticity of Tightly Entangled Solutions of Semiflexible Polymers. *Physical Review E*, 58(2):R1237–R1240, 1998.

[17] E. A. Osborn. *Actin Remodeling in Motile Cells.* PhD thesis, Massachusetts Institute of Technology, 1998.

[18] O. Pelletier, E. Pokidysheva, L. S. Hirst, N. Bouxsein, Y. Li, and C. R. Safinya. Structure of Actin Cross-Linked with $\alpha$-Actinin: A Network of Bundles. *Physical Review Letters*, 91:148102, 2003.

[19] J. H. Shin, M. L. Gardel, L. Mahadevan, P. Matsudaira, and D. A. Weitz. Relating Microstructure to Rheology of a Bundled and Cross-Linked F-Actin Network in Vitro. *Proceedings of the National Academy of Sciences of the United States of America*, 101(26):9636–9641, 2004.

[20] M. Tempel, G. Isenberg, and E. Sackmann. Temperature-Induced Sol-Gel Transition and Microgel Formation in $\alpha$-Actinin Cross-Linked Actin Networks: A Rheological Study. *Physical Review E*, 54(2):1802–1810, 1998.

[21] D. H. Wachsstock, W. H. Schwarz, and T. D. Pollard. Affinity of $\alpha$-Actinin for Actin Determines the Structure and Mechanical Properties of Actin Filament Gels. *Biophysical Journal*, 65(1):205–214, 1993.

[22] D. H. Wachsstock, W. H. Schwarz, and T. D. Pollard. Cross-Linker Dynamics Determine the Mechanical Properties of Actin Gels. *Biophysical Journal*, 66(3):801–809, 1994.

[23] B. Wagner, R. Tharmann, I. Haase, M. Fischer, and A. R. Bausch. Cytoskeletal Polymer Networks: The Molecular Structure of Cross-Linkers Determines Macroscopic Properties. *Proceedings of the National Academy of Sciences of the United States of America*, 103(38):13974–13978, 2006.

[24] A. Weins, P. Kenlan, S. Herbert, T. C. Le, I. Villegas, B. S. Kaplan, G. B. Appel, and M. R. Pollak. Mutational and Biological Analysis of $\alpha$-Actinin-4 in Focal Segmental Glomerulosclerosis. *Journal of the American Society of Nephrology*, 16:3694–3701, 2005.

[25] A. Weins, J. S. Schlondorff, F. Nakamura, B. M. Denker, J. H. Hartwig, T. P. Stossel, and M. R. Pollak. Disease-associated $\alpha$-actinin-4 reveals a mechanism for regulating its F-actin binding affinity. *Proceedings of the National Academy of Sciences of the United States of America*, 104(41):16080–16085, 2007.

[26] J. Xu, W. H. Schwarz, J. A. Käs, T. P. Stossel, P. A. Janmey, and T. D. Pollard. Mechanical Properties of Actin Filament Networks Depend on Preparation, Polymerizaion Conditions, and Storage of Actin Monomers. *Biophysical Journal*, 74:2731–2740, 1998.

[27] J. Xu, D. Wirtz, and T. D. Pollard. Dynamic Cross-Linking by $\alpha$-Actinin Determines the Mechanical Properties of Actin Filament Networks. *Journal of Biological Chemistry*, 273(16):9570–9576, 1998.